Am J Cancer Res 2020;10(2):581-594
www.ajcr.us /ISSN:2156-6976/ajcr0107151

Original Article

Potent and broad anticancer activities of leaf extracts from *Melia azedarach* L. of the subtropical Okinawa islands

Kuniaki Nerome[1], Taku Ito-Kureha[2], Tiziana Paganini[2], Takao Fukuda[3], Yasuhiro Igarashi[3], Hiroto Ashitomi[4], Shinya Ikematsu[4], Tadashi Yamamoto[2]

[1]The Institute of Biological Resources, 893-2, Nakayama, Nago-shi, Okinawa 905-0004, Japan; [2]Cell Signal Unit, Okinawa Institute of Science and Technology Graduate University, Onna, Okinawa 904-0495, Japan; [3]Biotechnology Research Center and Department of Biotechnology, Faculty of Engineering, Toyama Prefectural University, 5180 Kurokawa, Imizu, Toyama 939-0398, Japan; [4]National Institute of Technology, Okinawa College, Henoko 905, Nago-shi, Okinawa 905-2192, Japan

Received August 6, 2019; Accepted January 23, 2020; Epub February 1, 2020; Published February 15, 2020

Abstract: Plant extracts have been traditionally used for various therapeutic applications. By conducting an initial screening of several subtropical plants, in this study, we evaluated the anticancer activities of *Melia azedarach L.* The extract from *Melia azedarach L.* leaves (MLE) show high cytotoxic effects on cancer cells and *in vivo* mouse and dog tumor models. During the initial screening, MLE showed strong antiproliferative activity against HT-29 colon, A549 lung, and MKN1 gastric cancer cells. In subsequent tests, using 39 human tumor cell lines, we confirmed the potent anticancer activities of MLE. The anticancer activity of MLE was also confirmed *in vivo*. MLE markedly inhibited the growth of transplanted gastric MKN1 cancer xenografts in mice. To elucidate the mechanism underlying the anticancer effects of MLE, MLE-treated MKN1 cells were observed using an electron microscope; MLE treatment induced autophagy. Furthermore, western blot analysis of proteins in lysates of MLE-treated cells revealed induction of light chain 3 (LC3)-II autophagosomal proteins. Thus, MLE appeared to suppress MKN1 cell proliferation by inducing autophagy. In addition, in the mouse macrophage cell line J774A.1, MLE treatment induced TNF-α production, which might play a role in tumor growth suppression *in vivo*. We also performed a preclinical evaluation of MLE treatment on dogs with various cancers in veterinary hospitals. Dogs with various types of cancers showed a mean recovery of 76% when treated with MLE. Finally, we tried to identify the active substances present in MLE. All the active fractions obtained by reverse-phase chromatography contained azedarachin B-related moieties, such as 3-deacetyl-12-hydroxy-amoorastatin, 12-hydroxy-amoorastatin, and 12-hydroxyamoorastaton. In conclusion, MLE contains substances with promising anticancer effects, suggesting their future use as safe and effective anticancer agents.

Keywords: Cancer, anticancer therapeutics, plant extracts, *Melia azedarach*, autophagy inhibitors

Introduction

The development of new anticancer agents is of great importance to public health. Recent progress in molecular oncology has led to the development of molecular-targeting technologies for cancer therapy, and various chemical and biological therapeutics have proven effective in improving patient survival [1, 2]. Typical examples include imatinib, gefitinib, and erlotinib, which inhibit the kinase activities of oncogenic receptor kinases. Despite the progress in anti-cancer therapeutics, cancer is the second leading cause of mortality globally. The World Health Organization estimates that, globally, 14 million people are suffering from cancer and cancer caused 9.6 million deaths in 2018. Japan is no exception and the number of cancer-related deaths in Japan increased from 295,864 in 2000 to 353,000 in 2010, an increase of ~1% per year [3].

Plant extracts have been used as traditional remedies and are sources of several anticancer drugs distributed worldwide [4]. Among the first drugs from plants used for the treatment of cancer are microtubule-targeting agents, taxanes, and vinca alkaloids, which include pacli-

taxel, vinblastine, and vincristine [5-7]. Paclitaxel was originally isolated from the bark of the Pacific Yew, and vinblastine and vincristine were extracted from the Madagascar periwinkle [7, 8]. Inhibitors of DNA topoisomerase I, such as topotecan and irinotecan (CPT-11), are synthetic analogs of the cytotoxic alkaloid, camptothecin (CPT), isolated from the bark and stems of the Chinese Happy Tree [9]. Several synthetic analogs of CPT have better aqueous solubility, lower toxicity, and greater antitumor efficacy than the parent drug, among which irinotecan and topotecan are approved for clinical use [9, 10].

In this study, we purified and characterized potential anticancer compounds extracted from the leaf of the *Melia* tree (*Melia azedarach* L.) collected from the mainland of the Okinawa region. By exploring over 2,000 subtropical plants, we successfully discovered several plants that contain compounds with remarkable anticancer activity against three human tumor cell lines, colon HT-29, lung A549, and gastric MKN1. Among these plants, we chose the *Melia* tree for further studies on the basis of the strong anticancer activity of its compounds *in vitro* and *in vivo*.

Materials and methods

Preparation of MLE

The *Melia* leaves, obtained from Nago Municipality (Okinawa, Japan), were washed and dried at 65°C overnight. The samples were powdered and suspended in nine volumes of distilled water. The suspension was incubated at 60°C for 3 h and centrifuged at 9400 × *g* for 30 min. After centrifugation, the supernatant was dried by evaporation, and the dried material was suspended in distilled water at a concentration of 10.5 mg/ml; this suspension (crude extract) was tested for toxicity as described in the following section. The suspension was filtered through a 10-kDa cutoff membrane filter (Pellicon 2 Mini Filters; Millipore Corporation, Germany), and the filtrate was used as a 10.5 mg/ml sample of *M. azedarach* leaf extracts (MLE).

Toxicity test of the crude extract

To determine the fraction with most toxicity, the crude extract was filtered through various molecular weight cut-off membrane filters (Vivaspin 20: Sartorius); VS2091 (3,000 Da cut-off), VS2011 (5,000 Da cut-off), VS2001 (10,000 Da cut-off), VS2041 (100,000 Da cut-off), and VS2051 (300,000 Da cut-off). The toxicity of the six filtrate samples was tested in mice; 4-week-old female ddY (SPF) mice (n = 5; Japan SLC Co., Ltd.) were intraperitoneally administered 0.5 ml of the samples per day, diluted to 1.5 mg/ml. On day 170, the mice were euthanized by administering an excess of pentobarbital via intraperitoneal injection. The livers, spleens, kidneys, hearts, and lungs were then excised and weighed. The organs were fixed in 10% formalin (060-03845: Wako Pure Chemical Industries Ltd.) and sliced into 4-μm-thick sections, followed by hematoxylin and eosin (H&E) staining. All animal experiments were carried out in specific pathogen-free (SPF) conditions in accordance with the Fundamental Rules for Animal Experiments and the Guidelines for Animal Experiments Performed at The Institute of Biological Resources, published by the Animal Welfare and Animal Care Committee, including the Animal Ethics Committee of the Institute of Biological Resources (Okinawa, Japan).

Cell culture

The colon (HT-29), lung (A549), and gastric (MKN1) cancer cell lines (used for biological assays of MLE) were obtained from the Division of Molecular Pharmacology of Cancer Chemotherapy Center of the Japanese Foundation for Cancer Research (Tokyo, Japan). The HT-29 (JCRB 1383), A549 (JCRB 0076), and MKN1 (JCRB 0252) cancer cell lines (used for molecular mechanism analysis of MLE) were purchased from the Japanese Collection of Research Bioresources (JCRB) Cell Bank. The cells were cultured in Roswell Park Memorial Institute 1640 (RPMI 1640) medium (Gibco; Life Technologies) supplemented with 10% fetal bovine serum (FBS_F9423: Sigma-Aldrich). IMR90 and J774A.1 cells were purchased from the American Type Culture Collection and cultured in Dulbecco's modified Eagle's medium (DMEM) containing 10% FBS.

Measurements of cell growth inhibition

Cell growth inhibitory capacity of the plant extracts was measured as described previously [11-13]. Briefly, 10,000 cells were seeded into each well of 96-well plates in RPMI 1640 with 5% fetal bovine serum and allowed to attach overnight. The extracts were prepared in a

series of dilutions (10^{-1}-10^{-8}) in RPMI 1640 medium, and 100 µl of the extract was added to each well and incubated for 2 days. Subsequently, cell growth was determined according to the sulforhodamine B assay [14] as follows: the cells were washed five times with 1% acetic acid and incubated with 50 µl of 0.4% sulforhodamine B (in 1% acetic acid; Wako Pure Chemical Industries Ltd., Osaka, Japan). Then, 150 µl of 10 mM unbuffered Tris reagent (pH 10.5; Wako Pure Chemical Industries Ltd.) was added to each well, and the absorbance was measured at 525 nm using a standard plate reader. The concentration of test samples inhibiting 50% of the cell growth (GI50) was determined using the results of the above experiment.

Cell cycle analysis

MKN1 cells were cultured at an initial density of 2×10^5 cells/well in the presence or absence of MLE (105, 10.5, and 1.05 µg/ml) or mitomycin C (1 mg/ml, 139-18711: Wako Pure Chemical Industries Ltd.). At 1 and 2 days after initial seeding, the cells were ethanol-fixed and washed with PBS and incubated with 0.5 mg/ml RNase A (Sigma, R4875) for 30 min at 37°C. Cells were then stained with propidium iodide (Wako, 169-26281) and subjected to flow cytometry using a FACS Calibur (Japan BD Biosciences, Tokyo, Japan). FlowJo V10.4.2 (BD Biosciences) was used to analyze the results.

Immunoblot analysis

Cells were incubated with lysis buffer (50 mM Tris-HCl [pH 7.5], 150 mM sodium chloride, 1 mM ethylenediaminetetraacetic acid, 1% NP-40, and protease inhibitor cocktail [cOmplete Mini, Roche]). Proteins in the cell lysate were separated using sodium dodecyl sulfate-polyacrylamide gel electrophoresis and transferred to polyvinylidene difluoride membranes (Immobilon P, Merck Millipore). The membranes were then incubated with primary antibodies, and the immunoreactive proteins were visualized using anti-rabbit or anti-mouse IgG conjugated to horseradish peroxidase (RPN1231-2ML: GE Healthcare), followed by detection using an Enhanced Chemiluminescence (ECL) Detection System with film (GE Healthcare). The primary antibodies used were as follows: Anti-LC3 (light chain 3, PM036) was purchased from Medical & Biological Laboratories Co., Ltd. Anti-cleaved caspase 3 (Asp 175, clone 5aIE, #9664S), anti-cleaved poly-ADP ribose polymerase (PARP) (Asp 214, human-specific, #9541S), and anti-glyceraldehyde 3-phosphate dehydrogenase (GAPDH, rabbit mAb 14C10, #2118L) were purchased from Cell Signaling Technology Japan, K.K. (Tokyo, Japan).

Tumor formation assay

MKN1 cells (10^6 cells) were subcutaneously injected into BALB/c Slc-*nu/nu* (SPF) female mice (5 weeks old, Japan SLC, Inc.). When tumor sizes reached 50-150 mm^3, the mice were orally administered 0.5 ml MLE (1.5 mg/ml) every 4 days over a 3-week period. Tumor growth and body weight were monitored daily. Tumor volumes were determined using the standard formula: $V = 4\pi ab^2/3$ (V: tumor volume, 2*a: the major axis, 2*b: the minor axis).

Transmission electron microscopy (TEM)

Cells were washed, fixed in 2.5% glutaraldehyde for 30 min at 25°C, treated with 2% osmium tetroxide, dehydrated in a graded series of ethanol baths, infiltrated, and embedded in resin. Then, 50-nm-thick sections were cut using a Leica EM UC6 Ultramicrotome (Leica Microsystems), followed by staining with 4% uranyl acetate and 2% lead citrate, and visualization by TEM using a JEOL JEM-1230R electron microscope (JEOL, Ltd.) at an accelerating voltage of 100 kV.

Structure analysis of constituents in MLE

MLE (2 g/100 mL) was fractionated by C_{18} reversed-phase chromatography with 0.1% formic acid/acetonitrile (ACN) using a six-step gradient (20, 30, 40, 50, 60, and 70% ACN (v/v)). Six fractions were obtained (AF28, AF37, AF46, AF55, AF64, and AF73). Each fraction was evaporated and dried to obtain 2044, 53.6, 56, 9.1, and 3.3 mg of AF28, AF37, AF46, AF55, and AF64, respectively. No significant amount of material was recovered from the AF73 fraction. The fractions with anti-proliferative activity were subjected to high-performance liquid chromatography (Cosmosil AR-II, 20 × 250 mm) using a 0.1% formic acid/methanol (MeOH) gradient (MeOH concentration: 50% for 0-5 min, 50-55% for 5-9 min, 55% for 9-15 min, 55-70% for 15-22 min, and 70% for 22-27 min) to yield compounds with possible biological activities. The structures of the isolated compounds were

Table 1. Comparison of anticancer activity between MLE and Mitomycin C

Initial screening of anticancer compounds using three tumor cell lines			
Tumors	Cell lines	GI50* of crude extract from Melia tree leaf (μg/0.1 ml)	GI50* of Mitomycin C (μg/0.1 ml)
Lung cancer	A549	1.50	0.29
Colon cancer	HT-29	0.31	0.31
Gastric cancer	MKN1	1.30	1.42

*GI50: concentration inhibiting 50% of cell growth.

analyzed using nuclear magnetic resonance (NMR) spectroscopy and mass spectrometry (MS).

Statistical analysis

Statistically significant differences between groups were determined using Student's t-test, Wilcoxon test, or a SAS mixed procedure. *P*-values less than 0.05 were considered statistically significant. Values are expressed as the means of triplicate samples ± the standard error of the mean.

Preclinical evaluation of MLE in canine cancers in veterinary hospitals

Dogs were orally administered, once or twice a day, with 0.5, 1.0, and 1.5 ml MLE for dogs with < 5, 15-20, and > 20 kg body weight, respectively. Thirty-three dogs with various cancers from 15 veterinary hospitals in Niigata (2 Hospitals), Fukushima (1), Tokyo (2), Saitama (1), Shizuoka (2), Aichi (2), Gifu (1), Osaka (1), and Okinawa (3) prefectures were tested. Dogs were divided into test (n = 25) and placebo (only glycerin, n = 8) groups. Dogs previously treated with anticancer or immune compounds were excluded from this study. The following factors were evaluated: appetite, locomotor activity, body weight, tumor size, metastasis, and recurrence. The investigation was undertaken over a 6.5-month period. The test and placebo groups were clinically treated in accordance with the general guidelines and the Research Council guide for the care and use of animals of each hospital.

Results

Initial screening of anticancer compounds from subtropical plants

We searched for anticancer substances from more than 2,000 subtropical plants collected in Okinawa, and at least 10 plants were found to possess anticancer compounds. Particularly, crude extract from *Melia* tree leaves appeared to show high anticancer activity against colon (HT-29), lung (A549), and gastric (MKN1) cancer cells (**Table 1**). The concentrations of *Melia* leaf extract inhibiting 50% (GI50) of HT-29, A549, and MKN1 cell growth were 0.31, 1.50, and 1.30 μg/0.1 ml, respectively. These GI50 values were, except for that of A549 cells, principally similar to those of mitomycin C, which was used as the control anticancer drug. The crude extract of *Melia* tree leaves, however, unexpectedly appeared to contain toxic substances against mice. Therefore, the identification of toxic fractions was essential for the extract to be used for cancer treatment.

Identification of highly toxic components from the crude extract

When the crude extract of *Melia* tree leaf was intraperitoneally administered to mice, with varying doses, all 10 mice died within 2 h; pathological analysis revealed that their livers were largely swollen, and centrilobular necrosis and congestion was observed (**Table 2**). Splenic and myocardial necrosis were also observed. Although the livers did not show hemorrhage, hemorrhagic spots were observed in the heart (data not shown). However, mice that were orally administered the crude extract survived (**Table 3**). These results suggested that the crude extract contains substances that are toxic for mice when administered peritoneally.

To find the toxic fraction in the extract, the extract was filtered through various molecular weight cut off membrane filters, and the filtrates were tested for their toxicity against mice. Intraperitoneal administration of the 300-kDa cut-off filtrate, which contained only components of the crude extract under 300 kDa, resulted in 80% death of the treated mice (**Table 3**). The histopathological features in mice killed by the 300-kDa-cut-off filtrate were similar to those in mice killed by the crude extract, although splenic necrosis was observed only in mice administered the unfiltered crude

Table 2. Pathological changes in extract-treated mice

Administered extract	Cut-off molecular weights of the membrane filters						
	Unfiltered	300 kDa	100 kDa	10 kDa	5 kDa	3 kDa	Control (PBS)
Massive necrosis in the liver	-	-	-	-	-	-	-
Centrilobular necrosis in the liver	++	++	-	-	-	-	-
Congestion in the liver	+++	+++	-	-	-	-	-
Hemorrhage in the liver	-	-	-	-	-	-	-
Splenic necrosis	++	-	-	-	-	-	-
Myocardial necrosis	++	+	-	-	-	-	-

+++: Severe, ++: Moderate, +: Mild, -: No particular; PBS: Phosphate buffered saline.

Table 3. The mortality rate in mice administered various extracts of Melia tree leaf

Route of administration	Unfiltered	Cut-off molecular weights of the membrane filters					Control (PBS)
		300 kDa	100 kDa	10 kDa	5 kDa	3 kDa	
Intraperitoneal administration	*5/5	4/5	0/5	0/5	0/5	0/5	0/5
Oral administration	0/5	0/5	0/5	0/5	0/5	0/5	0/5

*Number of dead mice/number of mice in group; PBS: Phosphate buffered saline.

Table 4. Evaluation of anticancer activity against nine tumors consisting of 39 tumor cell lines

Tumors	Cell lines	GI50* (μg/0.1 ml)	Tumors	Cell lines	GI50* (μg/0.1 ml)	Tumors	Cell lines	GI50* (μg/0.1 ml)
Breast Cancer	HBC-4	1.50	Lung Cancer	NCI-H23	1.50	Kidney Cancer	RXF-631L	0.64
	BSY-1	0.11		NCI-H226	0.90		ACHN	1.50
	HBC-5	1.50		NCI-H522	0.97			
	MCF-7	1.50		NCI-H460	1.50			
	MDA-MB-231	0.90		A549	1.50			
				DMS273	0.24			
				DMS114	1.28			
Brain Cancer	U251	1.50	Skin Cancer	LOX-IMVI	0.88	Gastric Cancer	St.4	0.49
	SF-268	1.50					MKN1	1.50
	SF-295	0.44					MKN7	1.50
	SF-539	1.50					MKN28	1.50
	SNB-75	1.50					MKN45	0.52
	SNB-78	1.50					MKN74	0.77
Colon Cancer	HCC2998	0.82	Ovarian Cancer	OVCAR-3	0.88	Prostate Cancer	DU-145	1.50
	KM-12	1.34		OVCAR-4	1.28		PC-3	1.50
	HT-29	0.14		OVCAR-5	1.50			
	HCT-15	1.50		OVCAR-8	1.16			
	HCT-116	0.41		SK-OV-3	1.50			

*GI50: concentration inhibiting 50% of cell growth.

extract (**Table 2**). The toxicity was thus eliminated from unfiltered crude extract if the components over 100 kDa were removed. Death and histological abnormalities were not observed in mice intraperitoneally administered filtrates filtered through 100-, 10-, 5-, and 3-kDa cut-off membrane filters. Therefore, in all further experiments, only the 100-kDa cut-off filtrate was used as the MLE solution.

Growth inhibition activity of MLE against various cancer cell lines

To characterize the anticancer activity of MLE, the growth inhibitory effect of MLE against 39 cancer cell lines was examined (**Table 4**). MLE showed anticancer activity against a panel of 39 cancer cells with GI50 ranging from 0.11 μg/0.1 ml against the BSY-1 breast cancer cell

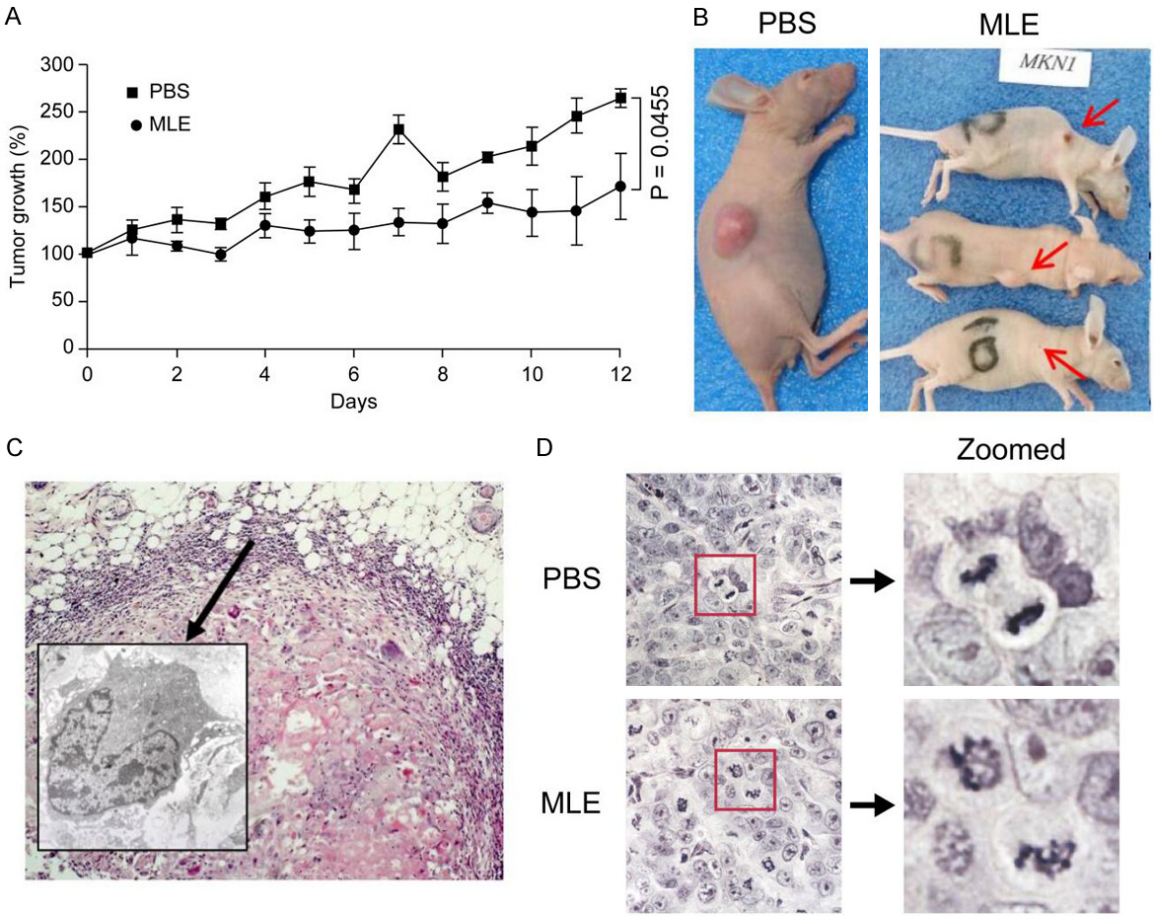

Figure 1. MLE suppresses tumor growth in the mouse xenograft model. Three mice (BALB/c Slc-*nu/nu*) were injected with 10^6 MKN1 cells (A-C) or HT-29 cells (D) subcutaneously and were orally administered with 0.5 ml of MLE solution (1.5 μg/ml) or PBS every 2 days. The administration started when tumors reached a volume of 50-150 mm^3. Average tumor volume was plotted with standard error (SE) against days after the administration. The tumor growth period between PBS- and MLE-administered mice were analyzed using SAS mixed procedure, and *P* value was determined (A). Mice were euthanized at 21 days after the administration, and the photographs of euthanized mice are shown; red arrows indicated tumors (B). Tumors of MLE-administered mice were histopathologically examined after H&E staining (C). The infiltrated mononuclear-like cells (indicated by arrow) were also examined with electron microscopy (inset in C). The thin sections of tumors were also Giemsa stained, and the M phase cells were analyzed (D).

line to 1.5 μg/0.1 ml in many other cancer cell lines. The anticancer activities of MLE against the 39 cancer cell lines showed significant differences, even among cell lines from the same cancers. As previously reported [13, 15], we also established a panel of these 39 cancer cell lines and developed a database of their chemosensitivities, in which various drugs were profiled for their "fingerprints" patterns of differential activity against these cell lines [15]. A significant correlation between a drug's fingerprint and its mode of action was observed. Based on the fingerprint database, the mechanism of anticancer activity of MLE was found to involve vacuolar-type H^+ ATPase inhibition because the fingerprint pattern of MLE was highly similar to that of bafilomycin, which is a well-known vacuolar-type H^+ ATPase inhibitor.

MLE efficiently prevented tumor growth in vivo

To determine whether the strong anticancer activities observed against various cancer cell lines can influence the tumor growth in an *in vivo* mouse model, we transplanted MKN1 gastric cancer cells into nude mice (**Figure 1**). After the size of the tumors reached 50-150 mm^3, the oral administration of MLE was started. The administration significantly reduced the growth of the tumor. In PBS-treated mice, the tumor size increased from 100% on the first day of the administration to 200% and 300% on days 7

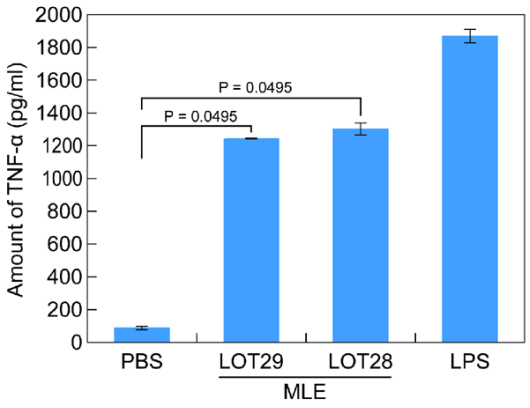

Figure 2. Activation of macrophages by MLE. J774A.1 mouse macrophage cells were treated with MLE, PBS, or LPS (Lipopolysaccharide from *E. coli* 055 served as a positive control) for 24 h. Cell culture supernatants were collected, and TNF-α levels were measured using ELISA (R&D Systems). Two different lots of MLE (LOT 28 and LOT 28) were compared. Statistically significant differences between group mean values were determined using the Wilcoxon test.

and 12, respectively. In contrast, tumors in MLE-administered mice were approximately two-fold smaller than those in PBS-treated mice at 12 days after the start of the administration. The result indicated that MLE treatment efficiently suppressed tumor growth (**Figure 1A**). We observed the effect of MLE administration until day 21. The difference in the appearance of tumors between MLE-administered mice and PBS-administered mice was significant (**Figure 1B**). Similar results were obtained in the mice transplanted with HT-29 colon cancer cells (data not shown).

Histopathological analysis of tumors from MLE-administered mice

Histopathological analysis of MKN1 cell-transplanted mice demonstrated the difference between the tumors from MLE-administered and PBS-administered mice. In H&E-stained sections of the tumors from MLE-administered mice, infiltrates of mononuclear-like cells were observed at the peripheral tumor sites. The dead gastric cancer MKN1 cells were enclosed with infiltrated cells, which showed structures characteristic of NK cells (**Figure 1C**).

HT-29 colon cancer cells were also analyzed. The observation of Giemsa-stained tumor slices revealed differences between images of M phase cells in MLE-treated and PBS-treated tumors. Cell-division images were more often observed in MLE-treated tumors than in control-treated tumors (**Figure 1D**). For quantitative analysis, we examined the frequency of metaphasic cells in the proliferating cell population. Proliferating cells were defined as Ki67-positive cells. The number of proliferating cells and metaphasic cells in five fields were counted under a microscope at 200x magnification. The percentage of metaphasic cells among the proliferating cells was about 2 times higher in tumors from PBS-treated mice than that in tumors from MLE-treated mice: 10.5% in PBS-treated mice and 4.7% in MLE-treated mice.

To examine the possibility of apoptosis induction by MLE treatment, TUNEL (terminal deoxynucleotidyl transferase dUTP nick-end labeling) staining of thin tumor sections was attempted. In MLE-treated gastric cancer tissue, much higher TUNEL-positive cells were observed than in PBS-treated ones (data not shown).

Activation of macrophages by MLE

The presence of infiltrated cells in tumors from MLE-administered mice suggested that MLE might activate immunological cells. To examine the possibility, J774A.1 mouse macrophage cells were treated with MLE, and the released tumor necrosis factor (TNF)-α was measured by ELISA. As expected, MLE markedly induced the release of TNF-α, an important antitumor cytokine, from the macrophages (**Figure 2**).

Suppression of MKN1 cell proliferation by MLE

To elucidate the tumor suppression activity of MLE, we investigated the effect of MLE on MKN1 cells *in vitro*. The number of MKN1 cells, treated with either 105 or 10.5 μg/ml of MLE, significantly decreased as compared to those treated with PBS (**Figure 3A**), which was consistent with the observed antitumor activity. In contrast, MLE hardly affected the proliferation of human normal fibroblast cells (IMR90; **Figure 3B**). Unexpectedly, we observed that the number of trypan blue positive MKN1 cells was unaltered for 2 days in the presence or absence of MLE (**Figure 3C**), suggesting that MLE did not affect the viability of MKN1 cells during the experimental period. Thus, MLE efficiently prevented tumor growth *in vivo* and *in vitro* while it did not directly cause cell death but suppressed cell proliferation.

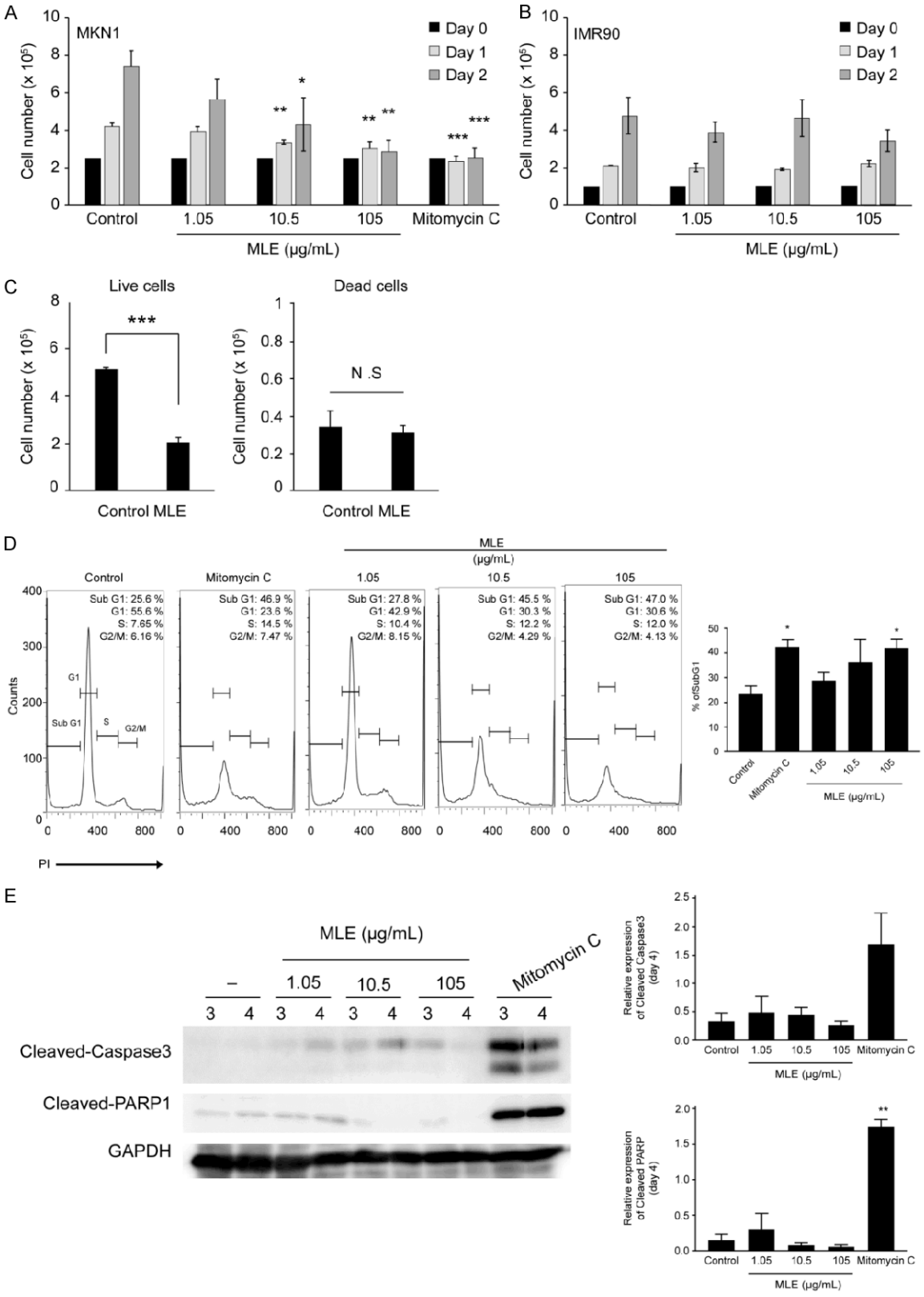

Figure 3. Effect of MLE on cellular proliferation *in vitro*. MKN1 cells (A) and IMR90 cells (B) were cultured in the presence or absence of MLE or mitomycin C at an initial density of 2 × 10^5 or 10^5 cells/well, respectively. Viable cells were counted 1 and 2 days after seeding. The MLE- or PBS-treated cells were further cultured for 2 days, and live and dead cells were counted using trypan blue staining (C). (D) Cell cycle analysis of MKN1 cells. Cell

cycle progression was analyzed using flow cytometry after treatment with MLE for 3 days. Data is representative of three independent experiments. The percentage of SubG1 phase cells from the replicates is also represented. (E) Immunoblot analysis of cleaved caspase 3 and cleaved PARP1. GAPDH serves as a loading control. Data are representative of two independent experiments. Bands were quantified by densitometry (right end). Statistically significant differences between group mean values were determined using the Student's *t*-test (***$P < 0.001$, **$P < 0.01$, and *$P < 0.05$).

To elucidate the mechanisms of the MLE-induced suppression, we first performed cell cycle analyses. Cell cycle progression was retarded, and the percentage of sub G1 fraction appeared to be increased by MLE treatment (**Figure 3D**). We examined the involvement of apoptosis in the retardation of the cell cycle. However, western blot analysis revealed no increase in cleaved caspase 3 and cleaved PARP1 expression in MLE-treated cells (**Figure 3E**) in contrast to the cells treated with mitomycin C, which is well-known to induce apoptosis. The result suggested that MLE affected cell proliferation by mechanisms other than apoptosis.

MLE induces autophagy

We then examined the intracellular structure of MLE-treated MKN1 cells using TEM. We observed autophagosome-like structures (**Figure 4A**). In addition, autophagy markers, LC3 I and LC3 II, were significantly expressed in MLE-treated MKN1 cells (**Figure 4B** and **4C**). These data suggest that cell growth suppression by MLE was due to autophagy of one of the mechanisms.

Preclinical evaluation of MLE treatment efficacy for canine cancer

To evaluate the efficacy of MLE treatment in higher vertebrates, we performed preclinical evaluations in 33 dogs with various cancers, including breast, liver, osteosarcoma, bladder, melanoma, mastocytoma, chromaffinoma, and thyroid carcinoma in 15 veterinary hospitals (**Figure 5B**). Dogs were divided into two groups (MLE: n = 25 and placebo: n = 8). We found that cancer progression was significantly ameliorated by MLE treatment in 76% of the dogs, compared to that in the placebo group (**Figure 5A**). Importantly, no abnormal and adverse reactions were observed in dogs. Thus, it could be concluded that MLE efficiently prevents cancer progression in dogs. These results suggested that MLE administration may be useful to treat cancer in humans and dogs. Furthermore, 14 major canine cancers, including hepatocellular carcinoma, osteosarcoma, and multiple myeloma, appeared to be markedly ameliorated (**Figure 5B**).

Identification of chemical compounds with anti-proliferative activity

To identify the constituents in MLE, a six-step gradient (20%, 30%, 40%, 50%, 60%, and 70% ACN v/v as eluate) separation process using C_{18} reverse-phase chromatography was carried out. We isolated five fractions (AF28, AF37, AF46, AF55, and AF64) and evaluated their antiproliferative effects. We found that the components of AF46, AF55, and AF64 had antiproliferative effects, whereas the components of AF28 and AF37 barely showed any effects (**Figure 6A**).

We next determined the structures of the compounds in MLE using NMR and MS. AF46, AF55, and AF64 all contained azedarachin B-related moieties (**Figure 6B**). AF46 contained 12-hydroxyamoorastatone and 12-hydoroxyamoorastatin; AF55 contained 12-*O*-acetylazedarachin B, meliatoxin B2, and toosendanin; and AF64 contained azedarachin B, 12-diacetyltrichilin, 3-diacetyltrichilin H, neoazedarachin B, and 7, 14 epoxyazedarachin B.

Discussion

In this study, we demonstrated the definite anticancer activity *in vitro* and *in vivo* of an extract from *M. azedarach L.* (*Melia* tree), found in the subtropical Okinawa. Plant extracts have been adopted for the treatment of various diseases [16, 17]. Particularly, limonoids have been investigated for possible use as medicinal remedies in humans and animals [5]. In this study, we showed that extracts of *M. azedarach L.* leaves contain compounds that are cytotoxic to cancer cells but not to normal cells (**Tables 1**, **4**; **Figure 3A**, **3B**). Similar cytotoxic activity was previously reported for the extracts from the

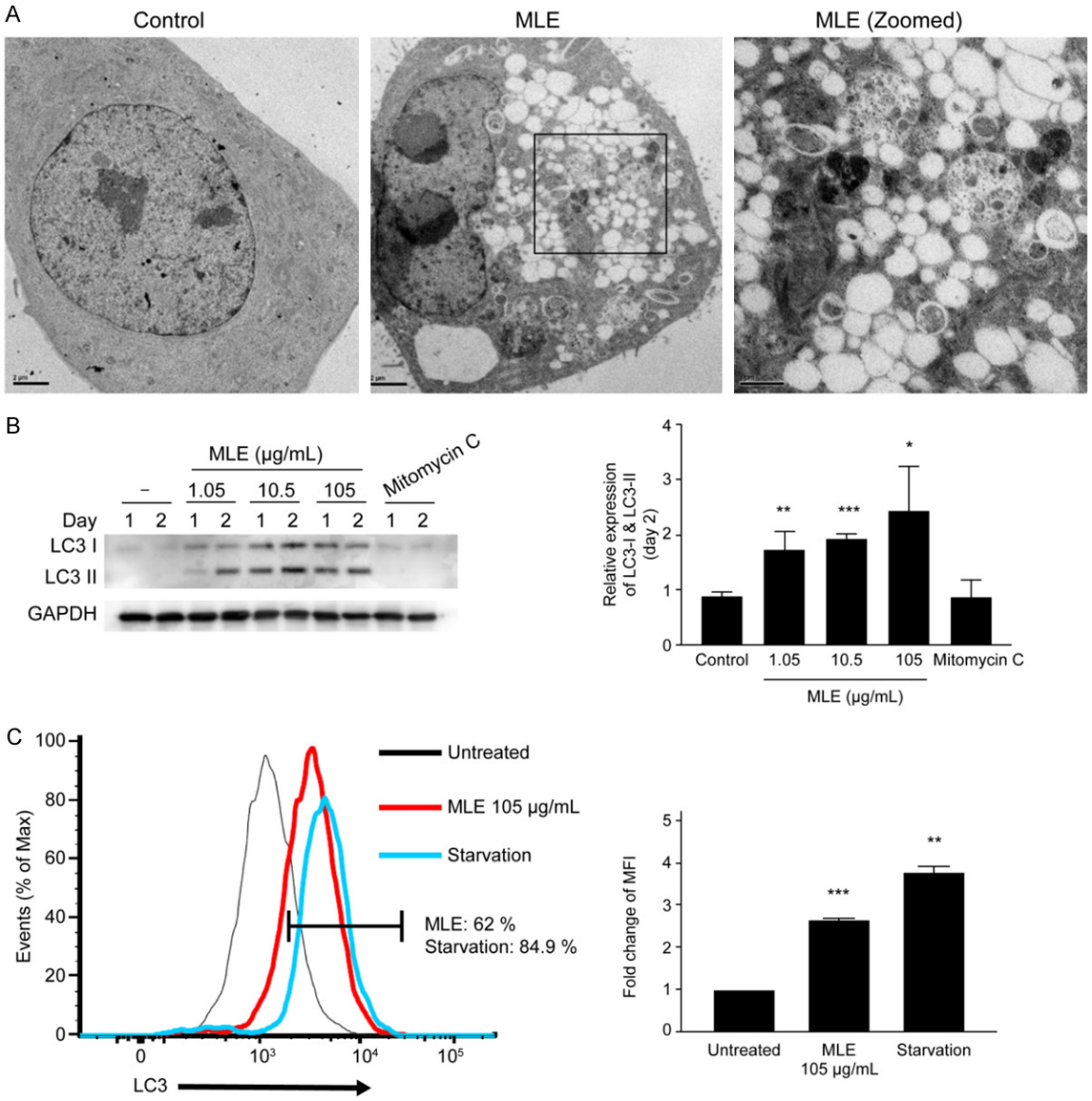

Figure 4. MLE induces autophagy in MKN1 cells. A. Representative images of MLE-treated MKN1 cells acquired by transmission electron microscopy. Autophagosomes highlighted in the square region are indicated via a zoomed-in image. Scale bars: 2 μm and 0.5 μm (zoomed). B. Immunoblot analysis of LC3. GAPDH serves as a loading control. Data is representative of three independent experiments. Bands were quantified by densitometry (right end). C. FACS analysis of LC3-expressing cells and fold change of Median fluorescence intensity (MFI). Cells that were serum-starved for 4 h were used as positive controls. Data from two independent experiments are represented. Statistically significant differences between group mean values were determined using the Student's *t*-test (***P < 0.001, **P < 0.01, and *P < 0.05).

bark, roots, and seeds of *M. azedarach L.* [18-22]. However, their underlying mechanism of activity remains elusive. We prepared the extract from leaves instead of bark, roots, or seeds of *M. azedarach L.* and showed that the extract induced autophagy in MKN1 gastric cancer cells (**Figure 4**). In contrast, toosendanin, which was identified in fraction AF55 in our study, was reported to induce apoptosis in U937 cancer cells [23]. In contrast, apoptosis induction was not detected in MLE-treated MKN1 cells (**Figure 3E**), but an increase in the number of TUNEL-positive cells was observed in tumors from MLE-treated mice (data not shown). These results suggest that MLE might inhibit cell growth depending on the type of cancer cells. Therefore, it was necessary to examine the effect of MLE on other cancer cell

A

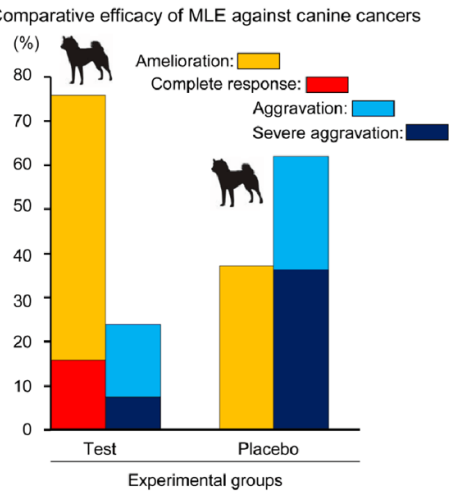

B Results of effective MLE treatment on canine cancers

Efficacy	No. of case	Cancers
Yes		
Complete response	4	• mammary gland cancer • mastocytoma • osteosarcoma, • malignant melanoma
Amelioration	15	• malignant melanoma • mammary gland cancer • hepatocellular carcinoma • osteosarcoma • metastatic mammary gland cancer • metastatic lung cancer • bladder transitional cell carcinoma • multiple myeloma, • prickle cell ameloblastoma • spleen hemangioma • fibro sarcoma • pulmonary tumor • malignant pheochromocytoma • thyroid cancer
No		
Aggregation	4	• hepatocellular carcinoma • basal squamous cell carcinoma • intraoral malignant melanoma • sarcoma angioplasticum
Severe aggregation	2	• metastatic lung cancer • metastatic mammary gland cancer

Figure 5. Effects of MLE on various cancers in dogs. A. Comparative efficacy of MLE against canine cancers; yellow, amelioration; red, complete response; light blue, aggravation; dark blue, severe aggravation. B. Classification of therapeutic efficacy of MLE on different canine cancers. The degree of MLE efficacy is shown on the left. Cases of treatment efficacy and MLE therapeutic efficacy on a large number of canine cancers are also described in the center and the right of the table.

types, which might reveal different mechanisms of cell death, such as apoptosis, necroptosis, or autophagy. Since various canine cancers were ameliorated by MLE treatment, different cytotoxic activities might have affected different cancers. Since we did not observe severe adverse effects in MLE-treated dogs, MLE might be useful as oral cancer therapeutics without remarkable side effects.

A few studies have suggested that autophagy induction is an effective strategy for cancer treatment [24]. However, various recently published studies indicate that autophagy induction helps the survival of adjacent cancer cells following chemotherapy [25, 26], and autophagy inhibitors have been used in combination with anticancer drugs [27-30]. Accordingly, the development of potential anticancer drugs with autophagy-inducing activity may be an effective strategy in cancer therapy [31].

An important observation--made in a study that addressed the mechanism of tamoxifen resistance--was that although tamoxifen induced autophagy [32], whether the autophagy was cytotoxic or rendered surviving cells tamoxifen-resistant was unclear [33, 34]. Eventually, tamoxifen-induced autophagy was shown to be cytotoxic to cancer cells due to autophagic degradation of cellular k-Ras protein [35]. Cells that lack k-Ras lose viability. In addition, in response to stress, c-Jun N-terminal kinase (JNK) was activated, phosphorylating B-cell lymphoma-2 (Bcl2) or BIM to dissociate Beclin from Bcl2, which led to the formation of an active Beclin1-VPS34 complex responsible for autophagy induction [36]. In summary, cellular stress can induce cell growth arrest or death. Some antitumor drugs that inhibit the mammalian target of rapamycin complex 1 (mTORC1), a negative regulator of the autophagic pathway, induce autophagy [37, 38]. Clarification of the intracellular mechanism by which MLE induces autophagy would help guide its therapeutic use.

Data showing that autophagy is regulated by cytokines in various biological contexts have been accumulating [39, 40]. For instance, TNF-α could play a role in stimulating autophagy, although the underlying mechanism has not been well established. The mechanisms might differ among cell types [41-44]. Conversely, autophagy affects the transcription of cytokine genes and secretion of cytokines [45, 46]. The autophagy inhibitor 3-methyladenine suppresses TNF-α transcription and secretion [47, 48]. Although we observed increased levels of TNF-α in MLE-treated macrophages *in vitro*, it is

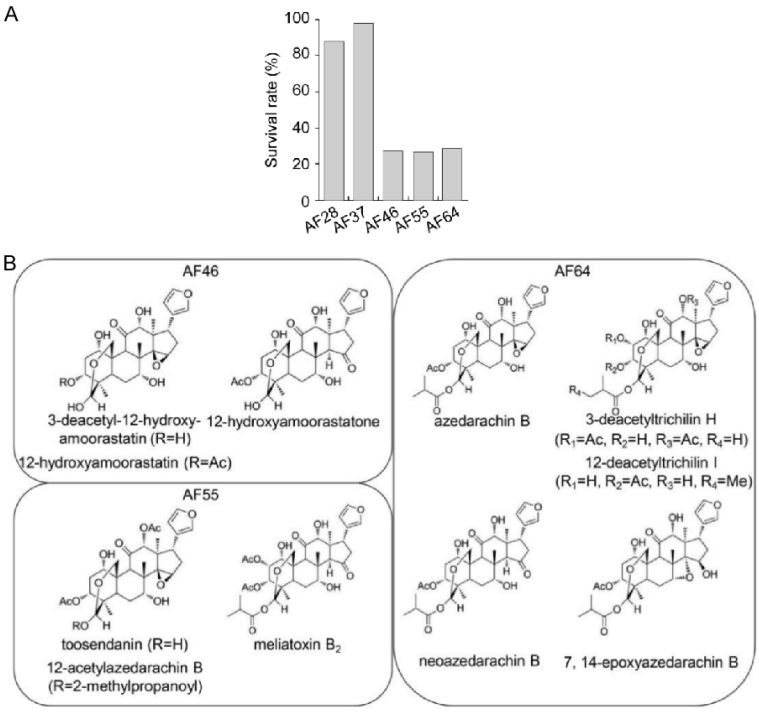

Figure 6. Structures of the constituents with antiproliferative activity in MLE. A. The antiproliferative activities of the five MLE fractions from the C_{18} column against HT 20 cells were evaluated as described in Materials and Methods (measurements of cell growth inhibition). B. Structures of the identified compounds in the fractions; AF46, AF55, and AF64, which showed strong antiproliferative effects.

unclear whether TNF-α induction by MLE is associated with a reduction of tumor growth *in vivo*. Further investigation of crosstalk between immunological cells and cancer cells would elucidate the mechanism of MLE-induced retardation of cancer development.

In this study, we not only identified MLE as an autophagy-inducing agent but also found that MLE treatment reduced the growth of multiple cancers in clinical tests with dogs and cats. Further studies should be conducted to examine whether cells that underwent autophagy following MLE treatment were killed. In addition, the development of therapeutic reagents against human cancers derived from MLE should be explored.

Acknowledgements

We thank Dr. T. Yoshikawa and Mr. S. Mukai (Institute of Biological Resources, Okinawa, Japan) for their skillful technical help and general support. We thank Ms. N. Ohmine (Okinawa Institute of Science and Technology Graduate University, Okinawa, Japan: OIST) and Dr. O. Elisseeva (Institute of Physical and Chemical Research, Kanagawa, Japan: RIKEN) for their technical support. We also thank Dr. K. Kuroda (Nihon University School of Medicine, Tokyo, Japan) for useful comments on the manuscript. We are grateful to the Kyoritsu Seiyaku Corporation (Tokyo, Japan) for their cooperation in the preclinical evaluation of MLE in veterinary hospitals. We also appreciate the Okinawa Institute of Science and Technology Graduate School for providing partial funding for this work. Authors appreciate Dr. R. Nerome (Institute of Biological Resources, Okinawa, Japan) for her generous supports for preparing the manuscript and figures.

Disclosure of conflict of interest

None.

Address correspondence to: Dr. Kuniaki Nerome, The Institute of Biological Resources, 893-2, Nakayama, Nago City, Okinawa 905-0004, Japan. Tel: +81-980-54-3376; Fax: +81-980-54-3457; E-mail: rnerome_ibr@train.ocn.ne.jp

References

[1] Scott AM, Wolchok JD and Old LJ. Antibody therapy of cancer. Nat Rev Cancer 2012; 12: 278-287.

[2] Sliwkowski MX and Mellman I. Antibody therapeutics in cancer. Science 2013; 341: 1192-1198.

[3] Katanoda K, Hori M, Matsuda T, Shibata A, Nishino Y, Hattori M, Soda M, Ioka A, Sobue T and Nishimoto H. An updated report on the trends in cancer incidence and mortality in Japan, 1958-2013. Jpn J Clin Oncol 2015; 45: 390-401.

[4] Surh YJ. Cancer chemoprevention with dietary phytochemicals. Nat Rev Cancer 2003; 3: 768-780.

[5] Ahn JW, Choi SU and Lee CO. Cytotoxic limonoids from *Melia azedarach var. Japonica*. Phytochemistry 1994; 36: 1493-1496.

[6] Dumontet C and Jordan MA. Microtubule-binding agents: a dynamic field of cancer therapeutics. Nat Rev Drug Discov 2010; 9: 790-803.
[7] Cragg GM. Paclitaxel (Taxol): a success story with valuable lessons for natural product drug discovery and development. Med Res Rev 1998; 18: 315-331.
[8] Johnson IS, Armstrong JG, Gorman M and Burnett JP Jr. The Vinca alkaloids: a new class of oncolytic agents. Cancer Res 1963; 23: 1390-1427.
[9] Martino E, Della Volpe S, Terribile E, Benetti E, Sakaj M, Centamore A, Sala A and Collina S. The long story of camptothecin: from traditional medicine to drugs. Bioorg Med Chem Lett 2017; 27: 701-707.
[10] Maeda M. Medical plants and folk remedies in Okinawa. Iseisya 1990.
[11] Monks A, Scudiero D, Skehan P, Shoemaker R, Paull K, Vistica D, Hose C, Langley J, Cronise P, Vaigro-Wolff A, et al. Feasibility of a high-flux anticancer drug screen using a diverse panel of cultured human tumor cell lines. J Natl Cancer Inst 1991; 83: 757-766.
[12] Yamori T, Sato S, Chikazawa H and Kadota T. Anti-tumor efficacy of paclitaxel against human lung cancer xenografts. Jpn J Cancer Res 1997; 88: 1205-1210.
[13] Yamori T, Matsunaga A, Sato S, Yamazaki K, Komi A, Ishizu K, Mita I, Edatsugi H, Matsuba Y, Takezawa K, Nakanishi O, Kohno H, Nakajima Y, Komatsu H, Andoh T and Tsuruo T. Potent antitumor activity of MS-247, a novel DNA minor groove binder, evaluated by an in vitro and in vivo human cancer cell line panel. Cancer Res 1999; 59: 4042-4049.
[14] Skehan P, Storeng R, Scudiero D, Monks A, Mcmahon J, Vistica D, Warren JT, Bokesch H, Kenney S and Boyd MR. New colorimetric cytotoxicity assay for anticancer-drug screening. J Natl Cancer I 1990; 82: 1107-1112.
[15] Yamori T. Panel of human cancer cell lines provides valuable database for drug discovery and bioinformatics. Cancer Chemother Pharmacol 2003; 52 Suppl 1: S74-S79.
[16] Balunas MJ and Kinghorn AD. Drug discovery from medicinal plants. Life Sci 2005; 78: 431-441.
[17] Newman DJ and Cragg GM. Natural products as sources of new drugs over the last 25 years. J Nat Prod 2007; 70: 461-477.
[18] Itokawa H, Qiao ZS, Hirobe C and Takeya K. Cytotoxic limonoids and tetranortriterpenoids from Melia azedarach. Chem Pharm Bull 1995; 43: 1171-1175.
[19] Takeya K, Quio ZS, Hirobe C and Itokawa H. Cytotoxic trichilin-type limonoids from Melia azedarach. Bioorg Med Chem 1996; 4: 1355-1359.
[20] Tada K, Takido M and Kitanaka S. Limonoids from fruit of Melia toosendan and their cytotoxic activity. Phytochemistry 1999; 51: 787-791.
[21] Ochi M, Kotsuki H, Ishida H and Tokoroyama T. Limonoids from *Melia-Azedarach* Linn. *Var. Japonica* Makino .II. the natural hydroxyl precursor of sendanin. Chem Lett 1978; 7: 99-102.
[22] Tan QG and Luo XD. Meliaceous limonoids: chemistry and biological activities. Chem Rev 2011; 111: 7437-7522.
[23] Zhang B, Wang ZF, Tang MZ and Shi YL. Growth inhibition and apoptosis-induced effect on human cancer cells of toosendanin, a triterpenoid derivative from Chinese traditional medicine. Invest New Drug 2005; 23: 547-553.
[24] Levy JMM, Towers CG and Thorburn A. Targeting autophagy in cancer. Nat Rev Cancer 2017; 17: 528-542.
[25] Ma XH, Piao S, Wang D, Mcafee QW, Nathanson KL, Lum JJ, Li LZ and Amaravadi RK. Measurements of tumor cell autophagy predict invasiveness, resistance to chemotherapy, and survival in melanoma. Clin Cancer Res 2011; 17: 3478-3489.
[26] Maycotte P, Aryal S, Cummings CT, Thorburn J, Morgan MJ and Thorburn A. Chloroquine sensitizes breast cancer cells to chemotherapy independent of autophagy. Autophagy 2012; 8: 200-212.
[27] Janku F, McConkey DJ, Hong DS and Kurzrock R. Autophagy as a target for anticancer therapy. Nat Rev Clin Oncol 2011; 8: 528-539.
[28] Ko A, Kanehisa A, Martins I, Senovilla L, Chargari C, Dugue D, Marino G, Kepp O, Michaud M, Perfettini JL, Kroemer G and Deutsch E. Autophagy inhibition radiosensitizes *in vitro*, yet reduces radioresponses *in vivo* due to deficient immunogenic signalling. Cell Death Differ 2014; 21: 92-99.
[29] Rangwala R, Chang YYC, Hu J, Algazy K, Evans T, Fecher L, Schuchter L, Torigian DA, Panosian J, Troxel A, Tan KS, Heitjan DF, Demichele A, Vaughn D, Redlinger M, Alavi A, Kaiser J, Pontiggia L, Davis LE, O'Dwyer PJ and Amaravadi RK. Combined MTOR and autophagy inhibition Phase I trial of hydroxychloroquine and temsirolimus in patients with advanced solid tumors and melanoma. Autophagy 2014; 10: 1391-1402.
[30] Rosenfeld MR, Ye XB, Supko JG, Desideri S, Grossman SA, Brem S, Mikkelson T, Wang D, Chang YYC, Hu J, McAfee Q, Fisher J, Troxel A, Piao SF, Heitjan DF, Tan KS, Pontiggia L, O'Dwyer PJ, Davis LE and Amaravadi RK. A phase I/II trial of hydroxychloroquine in conjunction with radiation therapy and concurrent and adjuvant temozolomide in patients with

newly diagnosed glioblastoma multiforme. Autophagy 2014; 10: 1359-1368.
[31] Thorburn A, Thamm DH and Gustafson DL. Autophagy and cancer therapy. Mol Pharmacol 2014; 85: 830-838.
[32] Bursch W, Ellinger A, Kienzl H, Torok L, Pandey S, Sikorska M, Walker R and Hermann RS. Active cell death induced by the anti-estrogens tamoxifen and ICI 164 384 in human mammary carcinoma cells (MCF-7) in culture: the role of autophagy. Carcinogenesis 1996; 17: 1595-1607.
[33] Gonzalez-Malerva L, Park J, Zou L, Hu Y, Moradpour Z, Pearlberg J, Sawyer J, Stevens H, Harlow E and LaBaer J. High-throughput ectopic expression screen for tamoxifen resistance identifies an atypical kinase that blocks autophagy. Proc Natl Acad Sci U S A 2011; 108: 2058-2063.
[34] Samaddar JS, Gaddy VT, Duplantier J, Thandavan SP, Shah M, Smith MJ, Browning D, Rawson J, Smith SB, Barrett JT and Schoenlein PV. A role for macroautophagy in protection against 4-hydroxytamoxifen-induced cell death and the development of antiestrogen resistance. Mol Cancer Ther 2008; 7: 2977-2987.
[35] Kohli L, Kaza N, Coric T, Byer SJ, Brossier NM, Klocke BJ, Bjornsti MA, Carroll SL and Roth KA. 4-Hydroxytamoxifen induces autophagic death through K-Ras degradation. Cancer Res 2013; 73: 4395-4405.
[36] Wei Y, Pattingre S, Sinha S, Bassik M and Levine B. JNK1-mediated phosphorylation of Bcl-2 regulates starvation-induced autophagy. Mol Cell 2008; 30: 678-688.
[37] Wander SA, Hennessy BT and Slingerland JM. Next-generation mTOR inhibitors in clinical oncology: how pathway complexity informs therapeutic strategy. J Clin Invest 2011; 121: 1231-1241.
[38] Benjamin D, Colombi M, Moroni C and Hall MN. Rapamycin passes the torch: a new generation of mTOR inhibitors. Nat Rev Drug Discov 2011; 10: 868-880.
[39] Harris J. Autophagy and cytokines. Cytokine 2011; 56: 140-144.
[40] Wu TT, Li WM and Yao YM. Interactions between autophagy and inhibitory cytokines. Int J Biol Sci 2016; 12: 884-897.
[41] Jia GH, Cheng G, Gangahar DM and Agrawal DK. Insulin-like growth factor-1 and TNF-alpha regulate autophagy through c-jun N-terminal kinase and Akt pathways in human atherosclerotic vascular smooth cells. Immunol Cell Biol 2006; 84: 448-454.
[42] Keller CW, Fokken C, Turville SG, Lunemann A, Schmidt J, Munz C and Lunemann JD. TNF-alpha induces macroautophagy and regulates MHC Class II expression in human skeletal muscle cells. J Biol Chem 2011; 286: 3970-3980.
[43] Sivaprasad U and Basu A. Inhibition of ERK attenuates autophagy and potentiates tumour necrosis factor-alpha-induced cell death in MCF-7 cells. J Cell Mol Med 2008; 12: 1265-1271.
[44] Djavaheri-Mergny M, Amelotti M, Mathieu J, Besancon F, Bauvy C, Souquere S, Pierron G and Codogno P. NF-kappa B activation represses tumor necrosis factor-alpha-induced autophagy. J Biol Chem 2006; 281: 30373-30382.
[45] Saitoh T, Fujita N, Jang MH, Uematsu S, Yang BG, Satoh T, Omori H, Noda T, Yamamoto N, Komatsu M, Tanaka K, Kawai T, Tsujimura T, Takeuchi O, Yoshimori T and Akira S. Loss of the autophagy protein Atg16L1 enhances endotoxin-induced IL-1 beta production. Nature 2008; 456: 264-U268.
[46] Nakahira K, Haspel JA, Rathinam VAK, Lee SJ, Dolinay T, Lam HC, Englert JA, Rabinovitch M, Cernadas M, Kim HP, Fitzgerald KA, Ryter SW and Choi AM. Autophagy proteins regulate innate immune responses by inhibiting the release of mitochondrial DNA mediated by the NALP3 inflammasome. Nat Immunol 2011; 12: 222-257.
[47] Crişan TO, Plantinga TS, van de Veerdonk FL, Farcaş MF, Stoffels M, Kullberg BJ, van der Meer JW, Joosten LA and Netea MG. Inflammasome-independent modulation of cytokine response by autophagy in human cells. PLoS One 2011; 6: e18666.
[48] Harris J, Hartman M, Roche C, Zeng SJG, O'Shea A, Sharp FA, Lambe EM, Creagh EM, Golenbock DT, Tschopp J, Kornfeld H, Fitzgerald KA and Lavelle EC. Autophagy controls IL-1 beta secretion by targeting pro-IL-1 beta for degradation. J Biol Chem 2011; 286: 9587-9597.